This article was downloaded by:
On: *25 January 2011*
Access details: *Access Details: Free Access*
Publisher *Taylor & Francis*
Informa Ltd Registered in England and Wales Registered Number: 1072954 Registered office: Mortimer House, 37-41 Mortimer Street, London W1T 3JH, UK

Liquid Crystals

Publication details, including instructions for authors and subscription information:
http://www.informaworld.com/smpp/title~content=t713926090

Laser-induced concentric colour domains in a cholesteric liquid crystal mixture containing a nematic azobenzene dopant

S. V. Serak; E. O. Arikainen; H. F. Gleeson; V. A. Grozhik; J. -P. Guillou; N. A. Usova

Online publication date: 11 November 2010

To cite this Article Serak, S. V. , Arikainen, E. O. , Gleeson, H. F. , Grozhik, V. A. , Guillou, J. -P. and Usova, N. A.(2002) 'Laser-induced concentric colour domains in a cholesteric liquid crystal mixture containing a nematic azobenzene dopant', Liquid Crystals, 29: 1, 19 — 26

To link to this Article: DOI: 10.1080/02678290110093778

URL: http://dx.doi.org/10.1080/02678290110093778

PLEASE SCROLL DOWN FOR ARTICLE

Full terms and conditions of use: http://www.informaworld.com/terms-and-conditions-of-access.pdf

This article may be used for research, teaching and private study purposes. Any substantial or systematic reproduction, re-distribution, re-selling, loan or sub-licensing, systematic supply or distribution in any form to anyone is expressly forbidden.

The publisher does not give any warranty express or implied or make any representation that the contents will be complete or accurate or up to date. The accuracy of any instructions, formulae and drug doses should be independently verified with primary sources. The publisher shall not be liable for any loss, actions, claims, proceedings, demand or costs or damages whatsoever or howsoever caused arising directly or indirectly in connection with or arising out of the use of this material.

LIQUID CRYSTALS, 2002, VOL. 29, NO. 1, 19–26

Taylor & Francis
Taylor & Francis Group

Laser-induced concentric colour domains in a cholesteric liquid crystal mixture containing a nematic azobenzene dopant

S. V. SERAK*, E. O. ARIKAINEN†, H. F. GLEESON†, V. A. GROZHIK‡,
J.-P. GUILLOU† and N. A. USOVA

Institute of Electronics of NASB, 22 Lagoiski Trakt, Minsk 220090, Belarus
†Department of Physics and Astronomy, The University of Manchester,
Manchester M13 9PL, UK
‡Institute of General and Inorganic Chemistry of NASB, 9 Surganova ul.,
Minsk 220072, Belarus

(*Received 16 December 2000; accepted 24 July 2001*)

The isothermal formation of concentric colour domains has been observed in a cholesteric mixture doped with 10 wt % of a photochromic nematic material. The host cholesteric mixture included the Merck materials BL131a and BL130, while the photochromic dopant was a mixture of 4-*n*-butyl-4′-*n*-alkoxyazobenzenes (BAAB). The helical pitch of the host cholesteric mixture was increased, as expected, on addition of the photochromic nematic material prior to irradiation with the molecules in the purely *trans*-configuration. On irradiation with low power (0.6 mW) argon ion laser light, *cis*-isomers formed within the interaction region and concentric colour domains appeared. Selective reflection from the colour domains occurred in the 400–560 nm spectral range. The coloured domains persisted in the time period following irradiation and extended beyond the interaction region because of diffusion of the *cis*-isomers. Using the diffusion equation, an expression has been obtained for the average concentration of *cis*-isomers in each of the coloured domains and the dependence of the reflection wavelength upon the concentration of *cis*-isomers has been determined.

1. Introduction

The ability of cholesteric structures to change their pitch reversibly due to a conformational *trans*–*cis* isomerization of the azo-fragment −N=N− is the basis for the operation of a number of optical devices featuring switching or memory effects [1–15]. The azo fragment can be a structural part of the chiral molecules themselves, or contained within dopants in a liquid crystalline matrix. UV irradiation or short wavelength laser illumination can stimulate the transition of rod-shaped *trans*-molecules to bent-shaped *cis*-molecules, a phenomenon known to reduce the stability of liquid crystalline phases. Doping a cholesteric liquid crystal with a photochromic nematic azo compound that initially exists in the ground state in the form of *trans*-isomers, results in a shift of the selective reflection band of the host to a longer wavelength region, an optical effect caused by an increase of the helical pitch. Photo-irradiation of such doped mixtures causes *cis*-isomers to form, which leads to the opposite effect—a reduction of the helical pitch and a shift of the reflection band towards shorter wavelengths [1, 10, 11, 16]. It is known that a build-up of *cis*-isomers even in small amounts (e.g. several wt % in nematic azo-benzenes [17]) stimulates an isothermal phase transition.

Isothermal phase transitions in the nematic liquid crystal formed from a mixture of 4-*n*-butyl-4′-*n*-alkoxyazobenzenes (BAAB) have been reported previously [17]. That work showed that isothermal phase transitions took place on irradiation with low power (7 mW) Ar^+ laser radiation and that components of the mixture have long-lived *cis*-conformational forms. Isotropic ‘holes’ were observed to persist for several hours in a 5 μm thick device. When viewed via polarization microscopy, it was possible to observe active diffusion of *cis*-isomers from the excitation zone and an expansion of the isotropic ‘hole’ after irradiation. This paper reports an isothermal phase transition induced by irradiation from a very low power (0.6 mW) Ar^+ laser in a cholesteric liquid crystal doped with the same nematic photochromic material. The cholesteric host material was selected because of its relatively temperature independent pitch. Following irradiation, a pattern of concentric colour domains with different reflection wavelengths in the 400–560 nm spectrum range is seen to form in the sample and expand beyond the region of illumination

---

*Author for correspondence; e-mail: serak@inel.bas-net.by

Liquid Crystals ISSN 0267-8292 print/ISSN 1366-5855 online © 2002 Taylor & Francis Ltd
http://www.tandf.co.uk/journals
DOI: 10.1080/02678290110093778

as a result of diffusion of *cis*-isomers. The domains are all observed to have reflection wavelengths smaller than the reflection wavelength of the undoped cholesteric/nematic material. The influence of the *trans–cis* transitions of the photochromic dopant on the reflection band is described and the pattern of concentric coloured domains is explained in terms of a diffusion model.

2. Experimental

2.1. *Materials and sample preparation*

The cholesteric host material, supplied by Merck Ltd., UK, was an 85/15 wt % mixture of the materials BL131a and BL130, with a clearing point of 102°C and a smectic to cholesteric transition temperature below −40°C. The cholesteric host material was doped with 10 wt % of a room temperature photochromic nematic mixture, denoted BAAB. The BAAB mixture is formed from equal weight ratios of the $n=1$, 2 and 5 homologues of 4-*n*-butyl-4′-*n*-alkoxyazobenzene and has a nematic to isotropic transition temperature of 56°C. Structural formulae of the homologues and their phase transition temperatures are given in figure 1. The BL131a/BL130/BAAB mixture had a cholesteric to isotropic phase transition temperature of 93°C and, in common with the host cholesteric material, no smectic phases were observed close to room temperature. The cholesteric host mixture is designed by Merck Ltd to have a relatively temperature-independent pitch, a property that persists following the addition of the photochromic nematic azobenzene mixture. The average selective reflection wavelength of the BL131a/BL130/BAAB mixture varied linearly with temperture from approximately 635 nm at 20°C to 655 nm at 93°C, i.e. the rate of change of pitch with temperature, dP/dT, is positive. All experiments involving irradiation of the BL131a/BL130/BAAB mixture were carried out at room temperature. Prefabricated devices, also provided by Merck Ltd, were used to encapsulate the liquid crystals. The device substrates are coated with rubbed polyimide films to ensure a planar orientation, and the thickness of liquid crystal layer was nominally 5 μm.

2.2. *Experimental methods*

Three methods were employed to determine the peak selective reflection wavelengths of the samples, depending on the area occupied by the reflecting region of interest. For large, uniform areas (>1 mm^2), absorption spectra were recorded on a Cary UV-Vis spectrophotometer. Alternatively, reflection spectra were measured by a specially designed reflection spectroscopy apparatus linked to an Olympus BH2-UMA reflection microscope. The UV-Vis spectrometer has a superior wavelength range and the reflection band can be associated with an absorption peak, but the sample illumination is relatively wide angle, causing broadening of the band. The reflection spectroscopy apparatus illuminates the sample at near-normal incidence, but the wavelength range is restricted to visible wavelengths (approximately 450 to 650 nm). Rapid determination of the selective reflection wavelength in small areas of the sample, of dimension around 100 μm and on a time scale faster than the relaxation time of the light-induced phenomena, could not be performed by either apparatus. Thus, wavelength analysis of the small concentric domains formed in the liquid crystal following irradiation was performed by analysis and colour matching of the image of the liquid crystal texture; this was recorded using a digital camera (JVC TK-C1381).

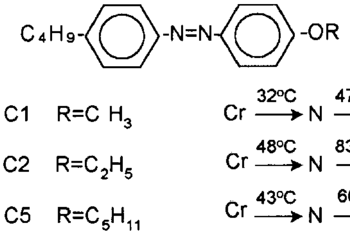

Figure 1. Structures and phase transition temperatures of the 4-*n*-butyl-4′-*n*-alkoxyazobenzene homologues.

In analysing the origin of the change of selective reflection from the photochromic cholesteric/nematic mixture, it was considered possible that the refractive index of the system was changed by irradiation. Since the wavelength of the selective reflection peak, λ_p, is related to the average refractive index, $\bar{n}=(n_o+n_e)/2$, and the helicoidal pitch of the system, p, through the equation [18],

$$\lambda_p = \bar{n}p \qquad (1)$$

a change in the selective reflection wavelength can be caused by changes in either the refractive index or the pitch. The refractive indices of the samples studied were measured using a commercial Abbe refractometer (Bellingham and Stanley Ltd.) at a wavelength of 590 nm over the temperature range 23–80°C. The cholesteric sample was aligned in a planar geometry, with the optic axis perpendicular to the faces of the refractometer prisms, by rubbing the surfaces of the prisms with a PVA solution. The use of this technique to measure the refractive indices of cholesteric liquid crystals is well known [18]; the ordinary and extaordinary indices can be deduced from two orthogonally polarized measurements, one corresponding to n_o, the other a combination of n_o and n_e.

3. Results and discussion

Figure 2 shows the absorption spectrum of the BL131a/BL130/BAAB mixture, measured using the UV-Vis spectrometer, together with the reflection spectrum

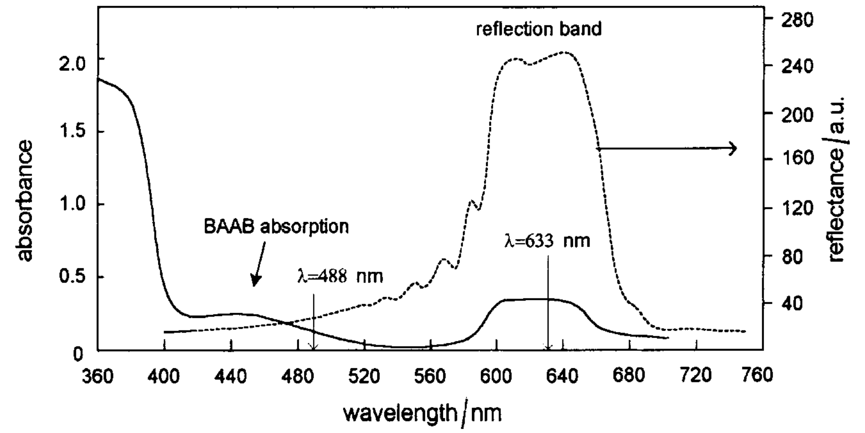

Figure 2. The absorption spectrum and reflection band of the BL131a/BL130/BAAB mixture at room temperature (20°C).

measured on the microscope apparatus. The selective reflection band of the mixture can be seen as a peak in the absorption spectrum in the region 600–655 nm. The absorption in the blue part of the spectrum is primarily due to the BAAB component in the mixture. The absorption coefficient of the cell was 30 cm^{-1} for light at 488 nm (the wavelength emitted by the Ar$^+$ laser). The reflection spectrum of the mixture shows only the reflection band of the cholesteric/nematic mixture and it can be seen that the peak of the reflection band coincides with a peak in the absorption spectrum. More detail of the interference fringes due to the finite sample thickness is apparent from the reflection spectrometer data.

A schematic illustration of the experimental arrangement used to investigate the temporal evolution of the isothermal phase transition induced in the photochromic BL131a/BL130/BAAB mixture is presented in figure 3. Light was incident on the sample from two laser sources: an Ar$^+$ laser was used for excitation ($\lambda = 488$ nm), while a He-Ne laser was chosen to probe the light-induced changes in the liquid crystal material as its wavelength (633 nm) is far from the BAAB absorption band. The power incident on the sample from the Ar$^+$ and He-Ne lasers was 0.6 and 0.2 mW, respectively. The laser light was focused by a lens of focal length 5 cm onto the cell to a spot 150 µm in diameter. Only light from the He-Ne laser transmitted by the device was incident on the photodetector, the output signal from which was processed by a computer. The probe beam wavelength lies in the centre of the selective reflection band of the mixture prior to excitation (see figure 2), so the sample initially reflects part of the light incident on it. Following illumination of the cell with Ar$^+$ laser light, and as a result of *trans–cis* isomerization, the planar-oriented liquid crystalline layer in the interaction region becomes isotropic. This phenomenon was observed via polarization microscopy as well being apparent from the increased intensity of the probe radiation at the cell exit. The insert in figure 3 shows the variation of the cell transmission with time. Here, the cell switching time, corresponding to the isotropic transition, is approximately 140 s for an Ar$^+$ laser power density of 3.4 W cm^{-2}.

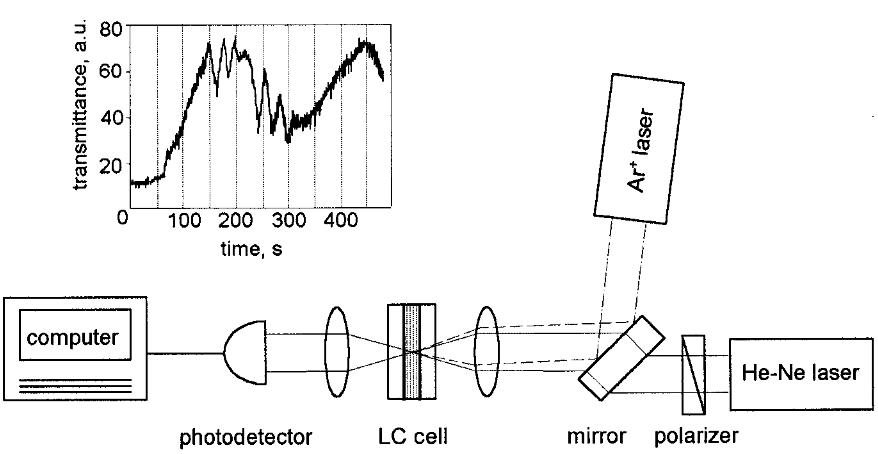

Figure 3. A schematic representation of the experimental unit used to study transmission kinetics in a cell filled with the BL131a/BL130/BAAB mixture. The insert shows the transmitted intensity of the photochromic cholesteric device as a function of time following illumination with the Ar$^+$ laser light, which is switched on at $t = 0$.

The switching time of a 5 μm thick cell filled with pure BAAB and placed between crossed polarizers has been investigated for comparison. In this case, the time taken to switch the nematic liquid crystal layer to the isotropic state using the same laser power density was 5 s. The much longer response time in the cholesteric mixture can be atrributed to the relatively low concentration of the photochromic species, as well as the enhanced liquid crystalline stability of the cholesteric mixture ($T_{\mathrm{NI}} = 56°\mathrm{C}$ for BAAB and $T_{\mathrm{ChI}} = 93°\mathrm{C}$ for the BL131a/BL130/BAAB mixture). It is known that He-Ne laser radiation can cause a reverse *cis–trans* isomerization of the photochromic molecules. At the power level used in these experiments ($\sim 1\ \mathrm{W\,cm^{-2}}$), the probe beam can stimulate the reverse transition of the layer from the isotropic state to the liquid crystal in several minutes [17]. This effect can be observed in the form of oscillations on the transmission versus time curve, shown in the insert in figure 3.

The appearance of the optically excited regions was examined in the viewing field of an Olympus BH2-UMA reflection microscope with white light illumination, following irradiation with light from the Ar^+ laser. Care was taken to maintain the illumination level and time well below those values which could induce a photochromic response in the mixture. Figure 4 depicts a pattern of six concentric colour domains induced in the chiral structure. The pattern emerged in the 20 s time period following the moment when the Ar^+ laser was switched off; the complex domain structure persisted for a lifetime of several seconds. Subsequently, the colour pattern broke down in such a way that domains with shorter helical pitch were transformed to domains with longer helical pitch, though the outer boundary of the whole structure did not change its position for several minutes.

The external dimensions of the domains were determined by their minimum diameter from the diagram shown in figure 4(*b*), and were approximately equal to (1) 150 μm, (2) 330 μm, (3) 570 μm, (4) 870 μm, (5) 1500 μm and (6) 1650 μm. The small size and short lifetime of the colour domains precluded the direct use of either the reflective spectroscopy apparatus or the UV-Vis spectrometer to determine the reflection wavelengths of the coloured regions. The reflection band wavelengths were therefore determined in the following manner. The irradiated sample was placed in the reflection microscope apparatus and a digitized video image of the colour domain in the viewing field was recorded. The colour of the video image was calibrated by recording images of the monochromatic light produced at the exit slit of the UV-Vis spectrophotometer. By changing the wavelength of monochromatic light coming from spectrophoto meter, the colour of the domains in the sample image were matched with the colour of the calibrated image. The following values of the reflection band wavelengths were obtained for each of the domains: (1) 400 nm, (2) 430 nm, (3) 465 nm, (4) 490 nm, (5) 530 nm and (6) 560 nm. For the principal field outside the illuminated area, the reflection band wavelengths measured by both the reflection spectroscopy and UV-Vis methods were equal to 625 nm (see figure 2). The error of determination of colour in the domains by this method certainly did not exceed the bandwidth of the selectively reflected light from the cholesteric structure, which is about 55 nm for this system, and was probably much less than this. The selective reflection wavelength reduces to a minimum at the centre of the domain pattern, with a maximum shift of 225 nm with respect to the non-irradiated sample. This shift is much larger than the 60 nm reported for a similar dye-doped cholesteric system [19].

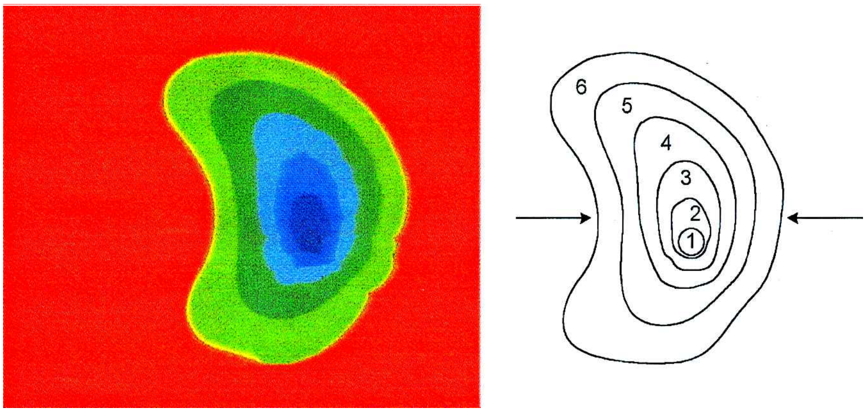

Figure 4. (*a*) A typical pattern of colour domains in a planar cell filled with the BL131a/BL130/BAAB mixture, emerging after irradiation with Ar^+ laser. (*b*) A diagram of the domain structure. The arrows on the diagram indicate the minimum radii measured and referred to in the diffusion calculations; the sample was at room temperature throughout.

As can be seen from equation (1), the reflected wavelength can be affected by a change of the helical pitch or a change in the refractive indices of the mixture, both of which can depend on the *cis*-isomer dopant concentration. If we assume that an increase in the *cis*-isomer concentration causes an order parameter change, it is important to consider that values of the refractive indices in different domains may be different. In the BL131a/BL130/BAAB mixture, the refractive indices n_o and n_e were found to be 1.6953 ± 0.0003 and 1.5108 ± 0.0001 respectively, at room temperature. The helical pitch in the non-irradiated cell was therefore estimated to be 390 nm. When the refractive indices were measured on the Abbe refractometer, the isotropic point of the mixture (93°C) could not be reached due to a technical limitation of the refractometer. The value of $\bar{n}$ calculated from the directly measured indices at 80°C ($n_e = 1.5093 \pm 0.0002$, $n_o = 1.6274 \pm 0.0006$), the highest point in temperature measured, was 1.5684 (± 0.0007). The variation of the average refractive index over the whole liquid crystal range can reasonably be assumed to be not higher than 0.03, since the average refractive index at 23°C in the mesophase is $\bar{n} = 1.6031$ and in the isotropic phase it is expected to be equal to: $n_{\text{iso}} = [(n_o^2 + 2n_e^2)/3]^{1/2} = 1.5747$. Thus, the variation in reflection wavelength associated with a refractive index change should not exceed 12 nm and such a small change in the refractive index could not alone account for the observed large change in reflection wavelength due to *trans–cis* isomerization. It therefore seems reasonable to suggest that the variation in the reflection wavelength is caused primarily by a variation in the helical pitch of the cholesteric mixture doped with BAAB. Further analysis of this proposal is provided in the next section.

4. Theoretical estimations and discussion

Irradiation with the Ar^+ laser causes a *trans–cis* isomerization of the azo-compound molecules incorporated in the chiral structure. The observations described in the preceding section can be modelled as follows, provided that the assumption is made that there is no selective adsorption of the *cis*-isomer on the solid surface, a process that takes place due to the higher polarity of the *cis*-isomer in comparison with the *trans*-isomer. In the experiment performed here, such an assumption is reasonable as the device substrates are coated with polyimide, though in cases where hydrophilic surface are used [20], such an assumption cannot be justified.

The non-stationary equation for the quantity of *cis*-isomers N_{cis} per unit volume can be written as:

$$\frac{\partial N_{cis}}{\partial t} = \frac{\beta K_0}{N_0 h\nu}(N_0 - N_{cis})U - \frac{N_{cis}}{\tau_c} + D\Delta N_{cis} \qquad (2)$$

where N_0 is the number of azo compound molecules per unit volume (before irradiation all of them are present in the *trans*-form), $U(x, y, t)$ is the radiation intensity, β is the quantum yield of photo-isomerization, K_0 is the absorption coefficient, $h\nu$ is the energy of a photon, τ_c is the *cis*-isomer lifetime, D is the diffusion coefficient and Δ is the Laplace operator. Consideration of the diffusion of *cis*-isomers in the cell is restricted to a two-dimensional case, because of the geometry of the experiment and the fact that the colour pattern lies in the plane of the cell. Then, the Laplace operator takes the form: $\Delta = \partial^2/\partial x^2 + \partial^2/\partial y^2$. This inherently implies that the *cis*-isomer concentration along the z-direction (normal to the glass substrates of the device) is constant. If $N_{cis} \ll N_0$, equation (2) takes the simplified form:

$$\frac{\partial N_{cis}}{\partial t} = \frac{\beta K_0}{h\nu}U - \frac{N_{cis}}{\tau_c} + D\Delta N_{cis}. \qquad (3)$$

Let the laser be switched on at a time $t = 0$ and switched off at time $t = t_1$, then $U(x, y, t) = 0$ when $t < 0$, or $t > t_1$, and $U(x, y, t) = U_0 f(x, y)$ when $0 < t < t_1$. Solving equation (3) for the initial condition $N_{cis}(r, t = 0) = 0$, and the boundary conditions $|x| < \infty$, $|y| < \infty$, the distribution of the number of *cis*-isomers at the end of the irradiation period t_1 can be shown to be described by the formula:

$$N_{cis}(x, y, t) = \exp\left(-\frac{t_1}{\tau_c}\right)\frac{\beta K_0}{h\nu}\int_0^{t_1} d\tau \int_{-\infty}^{\infty}\int_{-\infty}^{\infty} \times \frac{U(\xi, \eta, \tau)}{4\pi D(t_1 - \tau)} \exp\left(-\frac{(x-\xi)^2 + (y-\eta)^2}{4D(t_1 - \tau)}\right) \times \exp\left(\frac{\tau}{\tau_c}\right) d\xi\, d\eta. \qquad (4)$$

For a Gaussian distribution of the radiation intensity in the plane of the cell, $U = U_0 \exp[(x^2 + y^2)/r_0^2]$, equation (4) gives:

$$N_{cis}(r, t) = \exp\left(-\frac{t_1}{\tau_c}\right)\frac{\beta K_0 U_0}{h\nu}\int_0^{t_1} \frac{r_0^2}{r_0^2 + 4D(t_1 - \tau)} \times \exp\left(-\frac{r^2}{r_0^2 + 4D(t_1 - \tau)}\right)\exp\left(\frac{\tau}{\tau_c}\right) d\tau \qquad (5)$$

where $r^2 = x^2 + y^2$. When the laser source is switched off the diffusion process is governed by equation (3) with $U = 0$. Solving this equation for the initial conditions given by expression (5), equation (6) is obtained:

$$N_{cis}(r,t)=\exp\left(-\frac{t_2}{\tau_c}\right)\frac{\beta K_0 U_0}{h\nu}\int_0^{t_1}\frac{r_0^2}{r_0^2+4D(t_1-\tau)+4Dt_2}\times\exp\left(-\frac{r^2}{r_0^2+4D(t_1-\tau)+4Dt_2}\right)\times\exp\left(\frac{\tau}{\tau_c}\right)\mathrm{d}\tau. \qquad (6)$$

Here, t_2 is the time between the moment when the laser is switched off and the moment of observation. The average concentration of *cis*-isomers corresponding to one domain of a ring shape with inner radius r_1 and outer radius r_2 can be found by integrating equation (6) with respect to r. Ultimately the following relationship is obtained:

$$\langle N_{cis}\rangle=\frac{\beta K_0 U_0}{h\nu}\frac{r_0^2}{r_2^2-r_1^2}\times\int_0^{t_1}\left[\exp\left(-\frac{r_1^2}{R^2}\right)-\exp\left(-\frac{r_2^2}{R^2}\right)\right]\times\exp\left(\frac{\tau-t_2}{\tau_c}\right)\mathrm{d}\tau \qquad (7)$$

where $R^2=r_0^2+4D(t_1+t_2)-4D\tau$. Equation (7) allows the relative average amount of *cis*-isomers $\bar{N}(r_1,r_2)=\langle N_{cis}\rangle/N_0$ in each concentric domain to be calculated. N_0, the amount of azo moieties per unit volume, can be estimated according to the formula $N_0=CN_A\rho/M$, where C is the concentration of the azo moiety, N_A is Avogadro's number, ρ is the density ($1\ \mathrm{g\,cm^{-1}}$) and M is the molar mass (approximately $300\ \mathrm{g\,mol^{-1}}$). N_0 is then equal to $2.2\times10^{19}\ \mathrm{cm^{-3}}$. Figure 5(*a*) shows the dependence of the reflection wavelengths measured from each of the concentric domains in figure 4 on the relative concentration of *cis*-isomers $\langle N_{cis}\rangle/N_0$ estimated using (7) and the following values: $U_0=3.4\ \mathrm{W\,cm^{-2}}$, $\beta\sim0.7$, $K_0\sim30\ \mathrm{cm^{-1}}$, $h\nu\sim4\times10^{-19}$ J, $\tau_c\sim15$ s, $D\sim10^{-6}\ \mathrm{cm^2\,s^{-1}}$, $t_1=140$ s, $t_2=20$ s [21].

It can be seen from figure 5(*a*) that the reflection wavelength (and therefore the helical pitch) decreases with increasing concentration of *cis*-isomers. Such an effect cannot be due to local heating since not only does the mixture have a very small absorption coefficient at 488 nm (see figure 2), but the pitch of the BL131a/BL130/BAAB *increases* slightly with temperature. To allow the light-induced decrease in pitch to be considered in the context of an increasing nematic component in the mixture, figure 5(*b*) shows the variation in the reflection wavelength of the chiral nematic/nematic mixture BL131a/BL130 with changing concentration of the nematic component BL130. As expected, the selective reflection wavelength increases with the nematic component concentration. The square point on both graphs corresponds to the selective reflection wavelength of the BL131a/BL130/BAAB mixture under investigation. The reflection wavelength is close to the value measured in a 75/25 mixture of BL131a/BL130. It is evident from the figure that there are concentrations of *cis*-isomers for which the reflection wavelength becomes smaller than the reflection wavelength in the pure chiral nematic. It has been reported previously that a dye-doped cholesteric system exhibited a dP/d$T>0$ with the dye in the pure *trans*-form, but a negative dP/dT with the dye in the pure *cis*-form [19]. It would appear that in the material reported here, the *cis*-isomers also induce a negative variation of pitch with temperature, and, given the large shift observed, the incorporation of a few wt% of *cis*-isomers in the mixture brings about considerable disordering of the cholesteric structure.

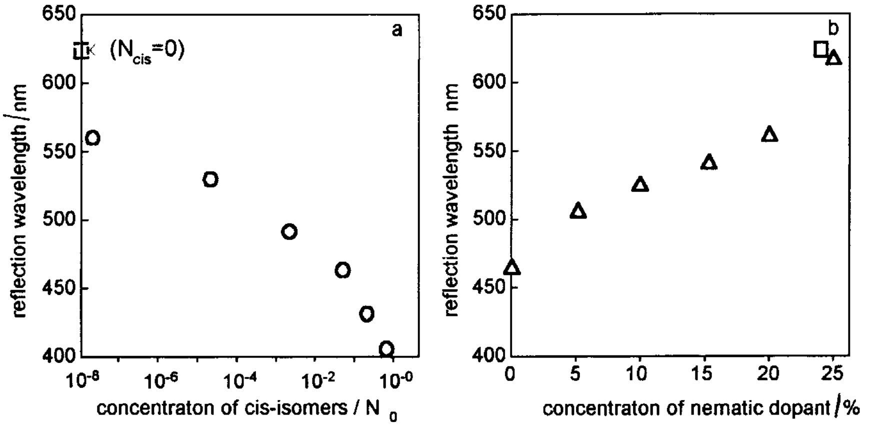

Figure 5. Variation of the reflection wavelength (*a*) with respect to the relative concentration of *cis*-isomers $\langle N_{cis}\rangle/N_0$ in the doped system, and (*b*) with the concentration of the nematic component BL130 in the undoped BL131a/BL130 mixture. The square point corresponds to the BL131a/BL130/BAAB mixture.

Further evidence that the light-induced change in cholesteric pitch in the BL131a/BL130/BAAB mixture is due to *cis–trans* isomerization of the BAAB molecules, rather than heating phenomena, can be deduced as follows. The behaviour of the pure BAAB mixture under excitation with Ar^+ laser radiation has been studied in our previous work [17, 22]. BAAB is characterized by an intense *trans–cis* isomerization, which results in the reduction of an order parameter and formation of an isotropic area in the region of irradiation. In the nematic BAAB mixture, the possibility that the isotropic area was of thermal origin was eliminated as follows. Firstly, the laser-induced isotropic region remained after cooling the cell in a refrigerator, spreading throughout the cell after irradiation was complete. Further, the characteristic times for thermal diffusion, τ_D, and mass diffusion of the isomers in the mixture BL131a/BL130/BAAB can be estimated by using the equation $\tau_D \approx r^2/\pi^2 D$ [23], where r is the distance between the centre of the illumination area and the boundary of the largest colour domain (~825 µm) and D is the corresponding diffusion coefficient. We assume the value $D \approx 10^{-3} \times \mathrm{cm}^2\ \mathrm{s}^{-1}$ for thermal diffusion and $D \approx 10^{-6}\ \mathrm{cm}^2\ \mathrm{s}^{-1}$ for mass diffusion of the isomers [23]. Then the characteristic thermal diffusion time is equal to 0.7 s, and the mass diffusion time is equal to 70 s. Given the time scale of the experiments here, the observed pitch change must be due to isomers and their diffusion rather than heating.

The origin of the anisotropy of the colour domain pattern that is apparent in figure 4 is not clear. It is possible that the orientation of the cell causes some of the observed anisotropy; if it is held vertical, diffusion will be enhanced in one direction and hindered in another. However, it is more likely that the anisotropic shape of the domains is a result of domain walls or inhomogeneities in the cell. It is well known that diffusion coefficents in liquid crystals are highly anisotropic, so it is most likely that the diffusion process is influenced by domain walls and alignment in the cell. Although such an effect certainly provides a qualitative explanation for the anisotropic nature of the colour domains, the phenomenon is worthy of further investigation.

Finally, it is worth commenting briefly on the fact that the colour domains observed in figure 4 are distinct ('quantized') even though the diffusion of the *cis*-isomers, which explains the change in reflection wavelength, is a continuous process. The quantization effect can be readily explained as a result of the strong parallel surface anchoring conditions present in the device used. Using the relationship (1) between the helical pitch, p, and reflection wavelength, λ_p, the number of half-pitches n_h in a parallel aligned cell of thickness d can be estimated to be $n_h = 2d\bar{n}/\lambda_p$. Calculating n_h for each ring it can be seen that the number of half-pitches in each domain is: {(39, 40, 41); (36, 37, 38); (33, 34, 35); (21, 32, 33); (29, 30, 31); (27, 28, 29)}; the numbers correspond to the domains in order, starting from the central spot and progressing outwards and the spread in number takes account of the accuracy with which λ_p is determined. Taking into account the accuracy of the reflection wavelength measurement, the number of pitches in neighbouring domains n_h varies by approximately 1.

5. Conclusion

This investigation has shown that, by using a low power Ar^+ ion laser (<1 mW) to irradiate a chiral nematic/nematic BL131a/BL130/BAAB mixture (which has a relatively temperature-independent helical pitch in which $dP/dT > 0$), it is possible to induce an isothermal phase transiton and to reduce the helical pitch by varying the *cis*-isomer concentration. Radial diffusion of the *cis*-isomers from the excitation region leads to the formation of several concentric coloured domains, with the helical pitch being progressively longer away from the irradiation region. A formula has been derived for the average concentration of *cis*-isomers in the domains based on the solution of the diffusion equation which explains the data presented.

This work has been carried out with support of the EEC through grant INTAS-BELARUS N97-0635 and the Engineering and Physical Science Research Council (grant GR/M/70858). The authors would like to thank Merck Ltd for provision of the chiral nematic materials and devices used in this study.

References

[1] Sackmann, E., 1971, *J. Am. chem. Soc.*, **93,** 7088.

[2] Haas, W. E., Nelson, K. F., Adams, J. E., and Dir, G. I., 1974, *J. electrochem. Soc.*, **121,** 1667.

[3] Udayakumar, B. S., and Shuster, G. B., 1983, *J. org. Chem.*, **58,** 4165.

[4] Suzuki, Y., Ozawa, K., Hosoki, A., and Ichimura, K., 1987, *Polym. Bull.*, **17,** 285.

[5] Vinogradov, V., Khizhnyak, A., Kutulya, L., Reznikov, Y., and Reshetnyak, V., 1990, *Mol. Cryst. liq. Cryst.*, **192,** 273.

[6] Petri, A., Brauchle, C. H., Leigeber, H., Miller, A., Weitzel, H.-P., and Kruzer, F.-H., 1993, *Liq. Cryst.*, **15,** 113.

[7] Janicki, S. Z., and Schuster, G. B., 1995, *J. Am. chem. Soc.*, **117,** 8524.

[8] Feringa, B. L., Huck, N. P. M., and Doren, H. A. V., 1995, *J. Am. chem. Soc.*, **117,** 9929.

[9] Yokoyama, Y., and Sagisaka, T., 1997, *Chem. Lett.*, 687.

[10] Kurihara, S., Kanda, T., Nagase, T., and Nonaka, T., 1998, *Appl. Phys. Lett.*, **73,** 2081.

[11] Yamaguchi, T., Inagawa, T., Nakazumi, H., Irie, S., and Irie, M., 2000, *Chem. Mater.*, **12,** 869.

[12] Kurihara, S., Nomiyama, S., and Nonaka, T., 2000, *Chem. Mater.*, **12,** 9.

[13] Tazuke, S., Kurihara, S., and Ikeda, T., 1987, *Chem. Lett.*, 911.

[14] Legge, C. H., and Mitchell, G. R., 1992, *J. Phys. D; Appl. Phys.*, **25,** 492.

[15] Ikeda, T., Miyamoto, T., and Kurihara, S., 1990, *Mol. Cryst. liq. Cryst.*, **188,** 207.

[16] Lee, H.-K., Doi, K., and Harada, H., 2000, *J. phys. Chem. B*, **104,** 7023.

[17] Grozhik, V., Gleeson, H., Serak, S., Watson, S., and Agashkov, A., 1998, *Mol. Cryst. liq. Cryst.*, **320,** 433.

[18] Gleeson, H. F., and Coles, H. J., 1989, *Mol. Cryst. liq. Cryst.*, **170,** 9, and references therein.

[19] Adams, J., Haas, W., and Wysocki, W., 1969, *Phys. Rev. Lett.*, **22,** 92.

[20] Ruslim, C., Komitov, L., and Matsuzawa, Y., 2000, *Jap. J. appl. Phys.*, **39,** 104, and references therein.

[21] For a typical value of D see, for example, Odulov, S. G., Reznikov, Yu. A., Soskin, M. S., and Khizhnyak, A. I., 1982, *Sov. JETP*, **82,** 1475.

[22] Watson, S. J., Gleeson, H. F., d'Emanuele, A., Serak, S. V., and Grhozhik, V. A., 1999, *Mol. Cryst. liq. Cryst.*, **331,** 375.

[23] De Gennes, P. G., and Prost, J., 1993, *The Physics of Liquid Crystals*, 2nd Edn (Oxford: Clarendon Press), p. 225.